Airflow Detection System Using a Stripped Silica Optical Fiber Sensor and Node MCU Microcontroller

Siti Halma Johari[1]*, Md Ashadi Md Md Johari[1], Muhammad Nur Ikhwan Ishak[1]

[1]Faculty of Electronics and Computer Technology and Engineering, Universiti Teknikal Malaysia Melaka, Hang Tuah Jaya, 76100 Durian Tunggal, Melaka, Malaysia

***Corresponding Author**

DOI: https://doi.org/10.47772/IJRISS.2026.101000570

Received: 26 October 2026; Accepted: 31 October 2026; Published: 10 November 2026

ABSTRACT

Airflow measurement is needed in ventilation, environmental monitoring and many industrial processes, yet the sensors commonly used for the job tend to be costly, bulky, or easily disturbed by electromagnetic noise, and many lose accuracy when the flow is weak. This paper describes the development and testing of an airflow detection system built around a stripped silica optical fiber sensor, with a NodeMCU microcontroller planned as the processing and wireless monitoring stage. A section of single-mode silica fiber was stripped of its coating, cleaved, and fusion-spliced to a fiber pigtail, and the joint was checked with a mini optical time domain reflectometer before testing. A portable mini fan, run at 10%, 50% and 100% of its output, supplied the airflow, while an optical power meter (OPM) recorded the transmitted optical power at 650 nm, 1310 nm and 1550 nm. Readings were taken at 3 s intervals over 15 s and repeated three times. At every wavelength the reading rose steadily with exposure time, and linear regression gave coefficients of determination between 0.9162 and 0.9976. The 650 nm source gave the most consistent linear behaviour (mean linearity 99.19%) and the clearest separation between airflow levels, the 1310 nm source performed best at low airflow, and the 1550 nm source produced the largest readings but was the least repeatable at 50% airflow. These results show that a simple, intensity-modulated stripped fiber can sense airflow reliably at low cost, and they point to 650 nm as a practical operating wavelength for a compact monitoring system.

Keywords: stripped silica optical fiber, airflow sensing, intensity modulation, microbending, optical power meter, NodeMCU

INTRODUCTION

Knowing how much air is moving, and how quickly that changes, matters in more places than is often appreciated. Heating, ventilation and air-conditioning (HVAC) systems depend on it to balance comfort against energy use, laboratories and clean rooms need it to keep contaminants under control, and industrial plants rely on it for cooling, drying and fume extraction. In each case the measurement has to be dependable, and in a growing number of applications it also has to be small, cheap and easy to connect to a monitoring network.

Conventional airflow instruments do not always meet these needs. Many existing systems are expensive, physically large or complicated to install, which makes them a poor fit for simple, low-cost deployments (Diez et al., 2024) (KMC Controls, 2025). Their accuracy can also suffer from electromagnetic interference (EMI) and from changes in the surrounding environment, and the problem tends to be worst at low flow velocities, where calibration and dynamic response are already difficult (Jiang et al., 2025). Some methods respond slowly, which limits their value for real-time monitoring. Together these shortcomings leave room for a sensor that is compact, inexpensive and immune to electrical noise while still reacting quickly to changes in flow.

Optical fiber sensors are well placed to fill this gap. Silica fiber is light, thin and non-conductive, so it is unaffected by EMI and can be placed close to motors, power cables and other noisy equipment. When the protective coating of a short length of fiber is removed, the guided light becomes more exposed to its

surroundings, and any mechanical disturbance at that point, such as vibration or bending caused by moving air, changes the amount of light that reaches the far end. Measuring that change with an ordinary light source and detector is far simpler than the interrogation required by more advanced fiber sensors, which keeps the cost of the whole system low (Murtaza & Senior, 2000).

This study set out to build and evaluate such a system. Its three objectives were (i) to develop an airflow detection system using a stripped silica optical fiber sensor, (ii) to analyse airflow from changes in the output optical power measured with an optical power meter (OPM), and (iii) to evaluate the performance of the system in terms of accuracy, linearity and response. Because the source wavelength affects how strongly a fiber reacts to bending, the sensor was tested at the three wavelengths most commonly used with silica fiber, namely 650 nm, 1310 nm and 1550 nm, under three airflow levels. The NodeMCU microcontroller is included in the system design as the stage that will process the detected signal and send it wirelessly for real-time monitoring.

LITERATURE REVIEW

Limitations of Conventional Airflow Sensing

Airflow sensing supports a wide range of applications, from building services and environmental monitoring to wearable devices, and demand is rising for sensors that are smaller and better integrated with digital systems. Jiang et al. (2025) note that despite steady progress, designers still struggle to balance sensitivity, structural design and system integration. At low velocities in particular, conventional methods can be let down by poor calibration, limited dynamic response and EMI, all of which degrade accuracy. Commercial experience points the same way: traditional airflow measurement is often criticised for its cost and for reliability problems once installed (KMC Controls, 2025).

The literature suggests three broad responses to these problems: making the sensing element itself more robust, using better signal processing, and linking sensors to wireless platforms so that data can be watched in real time. Low-cost Wi-Fi microcontrollers based on the ESP8266, such as the NodeMCU board, have become a common choice for the last of these because they combine processing and wireless connectivity on a single inexpensive module (Espressif Systems, n.d.).

Stripped Silica Fiber as an Intensity-Modulated Sensor

Fiber-optic sensors are attractive for airflow work because they are immune to EMI, compact and easy to distribute along a measurement path. Some fiber techniques, however, call for costly interrogation equipment. Intensity-modulated sensors avoid this. In the simplest arrangement a light source launches light into the fiber, a photodetector or power meter measures what arrives at the other end, and the measured intensity itself becomes the sensor output (Murtaza & Senior, 2000). The relationship between the measurand and the received intensity is usually captured as a calibration curve.

Removing the coating from a section of silica fiber, or reshaping it into a taper or U-bend, increases the interaction between the guided light and the surrounding medium. Parameters such as fiber diameter, bend radius and the length of the exposed region influence both sensitivity and response. A drawback of intensity-based schemes is that the output can also change for reasons unrelated to the measurand, including drift in the source and losses at connectors. Murtaza and Senior (2000) therefore recommend referencing or normalisation, for example taking ratios or relative measurements, so that the recorded change is tied more closely to the disturbance of interest.

Bending Loss as the Transduction Mechanism

When airflow strikes an exposed section of fiber it can cause vibration together with micro- and macrobending. Both forms of bending are well-known causes of attenuation, because they let part of the guided light leak out of the core or scatter (Jay, 2010). Microbending in particular has long been used on purpose as the transduction mechanism in fiber sensors, where a small mechanical deformation is converted into a measurable change in transmitted power (Lagakos et al., 1987). Reviews of distributed fiber sensing also confirm that optical

parameters, light intensity among them, change in a repeatable way under external vibration (Liu et al., 2016). This body of work supports the idea that airflow-induced vibration and deflection can be read out simply as a change in received optical power. The size of bending loss also depends on wavelength, since longer wavelengths are guided less tightly and are generally more sensitive to bends (Jay, 2010), which is why the wavelength chosen for the sensor deserves attention.

Fiber Preparation and Verification

The quality of a stripped fiber sensor depends heavily on how carefully the fiber is prepared. Stripping removes the protective polymer coating, and it has to be done without scratching or weakening the glass; mechanical strippers similar to copper wire strippers are widely used for this (Lee et al., 2011). The end of the fiber must then be cleaved. Most cleavers work on a scribe-and-tension principle, in which a hard blade scores the glass and controlled tension makes the crack run across the fiber to leave a flat end face (Jawad & Sultan, 2023).

The prepared fiber is usually joined to a pigtail, a short length of fiber with a factory-fitted connector at one end and a bare end at the other. Splicing a factory-terminated pigtail onto a fiber gives more consistent results than polishing a connector in the field (The Fiber Optic Association, n.d.). Fusion splicing, in which the two ends are aligned and welded with an electric arc, gives low loss and a joint almost as strong as the original fiber (Jawad & Sultan, 2023). The finished link can be checked with an optical time domain reflectometer (OTDR), which sends pulses down the fiber and analyses the Rayleigh backscatter to locate losses and faults (Azendorf et al., 2021) and with an OPM, whose calibrated photodiode sensor measures the average optical power at a set wavelength (Konstantatos et al., 2007).

Taken together, the literature shows that a stripped silica fiber read out by a simple source and detector should be able to sense airflow, but it says comparatively little about how the choice of source wavelength affects the linearity and repeatability of such a sensor when the flow level changes. This study addresses that question directly.

METHODOLOGY

Research Design

An experimental approach was used. The work was organised in three stages that matched the three objectives: building and verifying the sensor, recording the optical response to airflow at three wavelengths, and analysing the data for linearity and consistency. Figure 1 summarises the experimental workflow, from fiber preparation to the final optical power reading, and Figure 2 shows the procedure as a flowchart, including the check on splice loss that decided whether a sample could move on to testing.

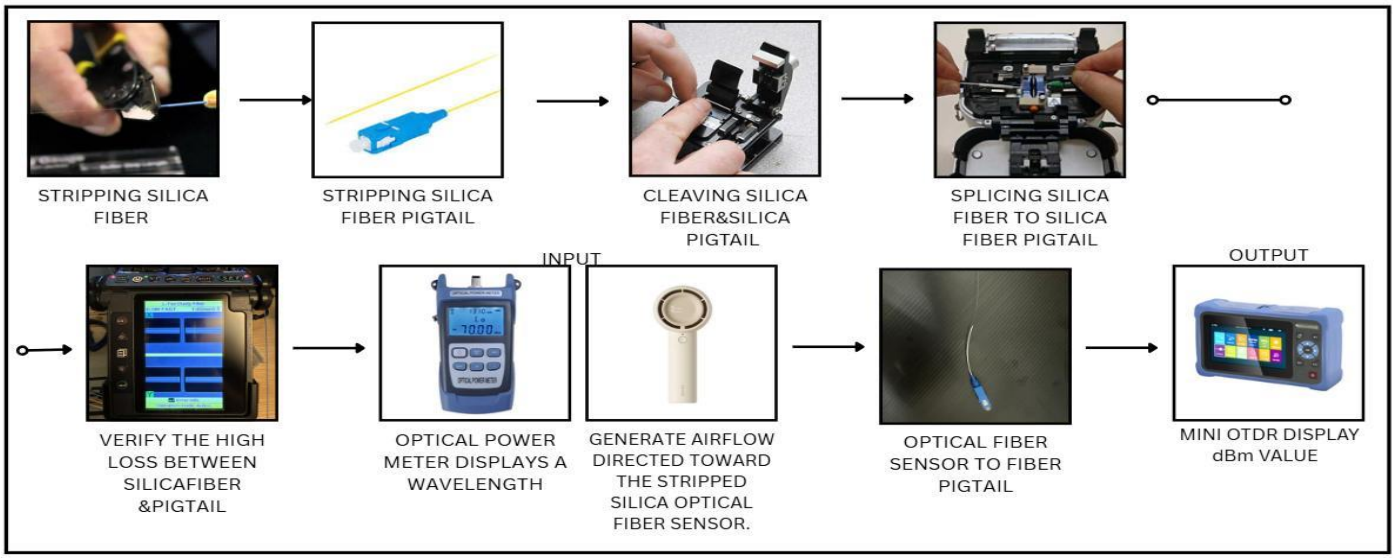

Figure 1: Block diagram of the experimental workflow

Tools were chosen with sustainability in mind as well as performance. A precise stripper and a good cleaver reduce broken fiber and failed splices, so less fiber and fewer splice sleeves are wasted. Checking the joint early with the OPM and mini OTDR prevents whole test runs from being repeated on a faulty sample. A handheld mini fan was used to generate airflow because it is cheap, draws little power and gives repeatable conditions without the need for a large wind tunnel. The equipment and its role are listed in Table 1.

Table 1: Equipment Used and Its Role in the Setup

Equipment	Role in the experiment
Single-mode silica optical fiber	Sensing element; the stripped section is exposed to the airflow
Optical fiber pigtail	Provides a connectorised, low-loss link between the sensing fiber and the instruments
Fiber stripper	Removes the polymer coating without damaging the glass cladding
Fiber cleaver	Produces a flat, perpendicular end face for low-loss splicing
Fusion splicing machine	Permanently joins the sensing fiber to the pigtail
Mini OTDR	Verifies splice quality and detects abnormal loss before testing
Optical power meter with light source	Launches light at 650, 1310 or 1550 nm and records the received optical power in dBm
Portable mini fan	Generates airflow at 10%, 50% and 100% of its output
NodeMCU (ESP8266) microcontroller	Planned processing and Wi-Fi stage for real-time monitoring

Sensor Fabrication

A short length of single-mode silica fiber was stripped of its coating to expose the cladding. Both the sensing fiber and the pigtail were then cleaved and joined with the fusion splicer. After splicing, the loss across the joint was checked on the mini OTDR. If the loss between the sensing fiber and the pigtail was not acceptable, the fiber was stripped, cleaved and spliced again, as shown by the loop in Figure 2. Only samples that passed this check were used for the airflow tests.

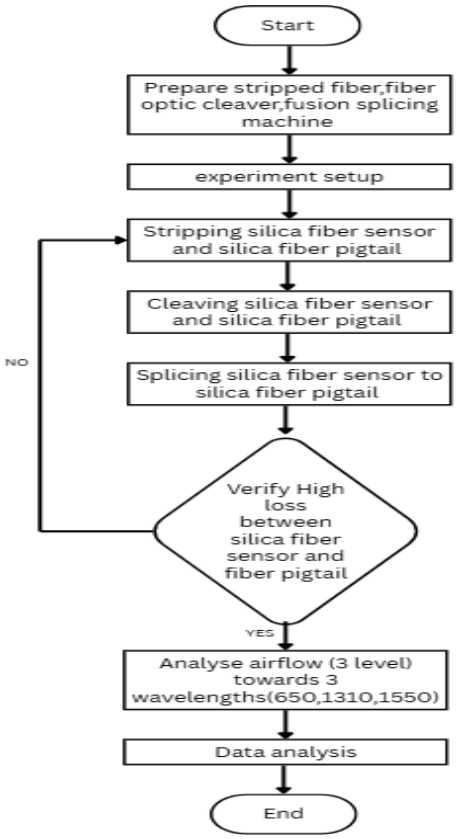

Figure 2: Flowchart of the experimental procedure

Experimental Setup and Procedure

The pigtail end of the sensor was connected to the OPM, which also served as the light source. The mini fan was placed at a fixed distance from the stripped section and pointed directly at it. Three airflow levels were tested, corresponding to 10%, 50% and 100% of the fan output (referred to as Levels 1, 2 and 3). These settings were used to investigate the relative optical response of the stripped silica fiber under different fan operating conditions rather than to quantify absolute airflow velocity. For each level, the optical power reading was noted at 3, 6, 9, 12 and 15 s after the airflow was applied. The whole sequence was repeated three times and then carried out again at each of the three source wavelengths. All other conditions were held constant, as listed in Table 2.

Table 2: Fixed Experimental Conditions

Parameter	Setting
Fiber type	Single-mode silica fiber, stripped section
Source wavelengths	650 nm, 1310 nm, 1550 nm
Airflow levels	10%, 50% and 100% of mini fan output
Fan-to-sensor distance	Fixed for all runs
Reading times	3, 6, 9, 12 and 15 s after airflow is applied
Repetitions	Three trials per condition
Ambient conditions	Room temperature, indoor laboratory

Data Analysis

For each combination of wavelength and airflow level, the mean of the three trials was calculated at every time point. A straight line, $y = mx + c$, was fitted to the mean readings against exposure time by least squares. The slope m describes how quickly the reading changes with time, and the intercept c gives the baseline level of the fitted line. Two measures were used to judge how well the response followed a straight line. The coefficient of determination (R^2) shows how closely the points sit on the fitted line, while linearity was expressed as the Pearson correlation coefficient multiplied by 100%, which is the square root of R^2 in percentage form. A value close to 100% indicates a response that is proportional and free of curvature over the measured range. The spread between the three trials was also examined as a simple indication of repeatability.

RESULTS AND DISCUSSION

Optical Power Response to Airflow

The mean OPM readings for all nine test conditions are given in Table 3. The values are reported exactly as displayed by the meter. A single pattern runs through the whole data set: at every wavelength and every airflow level, the reading increased steadily from 3 s to 15 s, and in most cases a stronger airflow gave a higher reading at a given time.

Table 3: Mean OPM Readings (dBm) of Three Trials at Each Exposure Time

Time (s)	650 nm			1310 nm			1550 nm		
	10%	50%	100%	10%	50%	100%	10%	50%	100%
3	3.29	4.13	6.15	10.99	12.63	13.99	13.15	13.25	14.04
6	4.00	7.03	7.73	12.77	14.02	14.59	14.58	14.99	15.07
9	6.53	8.26	9.73	15.22	16.29	15.55	16.13	17.21	16.50
12	8.12	10.48	11.75	18.01	18.28	18.11	17.83	18.18	17.76
15	11.23	12.65	13.30	20.12	21.70	20.35	20.32	23.70	20.13

At 650 nm the mean reading rose from 3.29 to 11.23 under 10% airflow and from 6.15 to 13.30 under 100% airflow. The same upward trend appeared at 1310 nm, where the 10% curve climbed from 10.99 to 20.12, and at 1550 nm, where it went from 13.15 to 20.32. The rise with airflow level is easy to explain. A stronger stream of air pushes harder on the bare fiber, so the vibration, deflection and microbending at the stripped section all

become larger, and these disturbances alter how much light is guided past the sensing region (Jay, 2010; Lagakos et al., 1987). The rise with time suggests that the fiber does not settle instantly. As exposure continues, the stripped section is driven into a more sustained state of oscillation and the effect on the transmitted light accumulates over the first several seconds. In particular, the propagation characteristics at 650 nm may differ from those at other wavelengths, potentially influencing the optical response to bending or vibration (Johari et al., 2022).

The overall level of the readings also depended clearly on wavelength. The 650 nm readings were the lowest throughout, the 1310 nm readings sat higher, and the 1550 nm readings were generally the highest. This ordering fits the expectation that longer wavelengths interact more strongly with bends in the fiber (Jay, 2010), although, as discussed below, a larger reading did not translate into a cleaner or more repeatable response.

Agreement between the three trials was generally good. At 650 nm the trial-to-trial standard deviation never exceeded 0.55, and at 1310 nm and 1550 nm it stayed below about 0.91 in all but one case. The exception was the third trial at 1550 nm, 50% airflow and 15 s, which read 30.10 while the other two trials read 20.90 and 20.10. That single value lifts the mean at this point to 23.70 and has a visible effect on the regression, as shown in the next section. Its size and isolation point to a momentary disturbance during that run, such as a slight movement of the fiber or a change in the fan position, rather than a real feature of the sensor's response.

Linear Response at Each Wavelength

Figure 3 plots the individual trials and their means against exposure time, together with the fitted lines, and Table 4 gathers the regression results. Every one of the nine conditions produced a strong linear fit, with R^2 no lower than 0.9162.

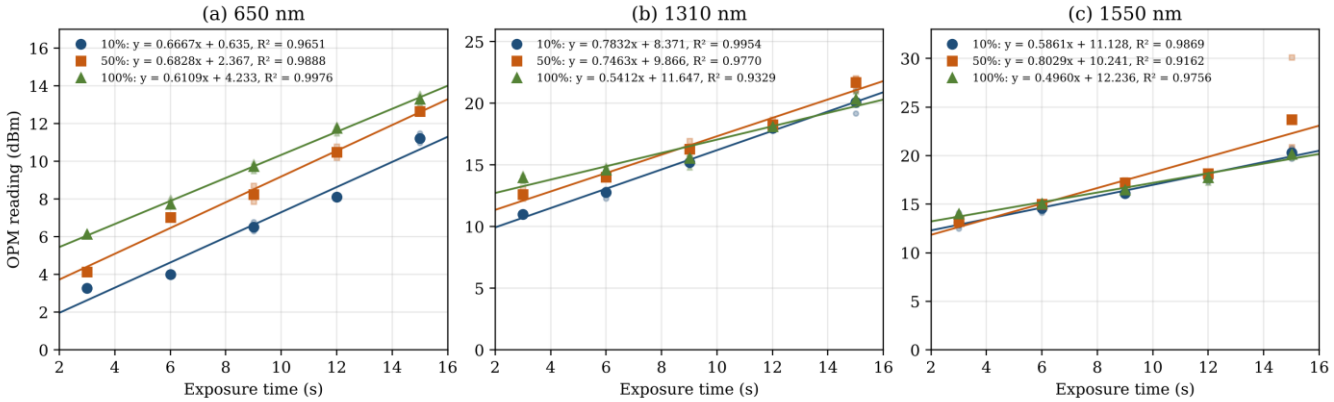

Figure 3: Sensor output against exposure time with linear fits at (a) 650 nm, (b) 1310 nm and (c) 1550 nm

Table 4: Linear Regression Results, R^2 and Linearity for Each Test Condition

Wavelength (nm)	Airflow (%)	Slope, m	Intercept, c	R^2	Linearity (%)
650	10	0.6667	0.635	0.9651	98.24
650	50	0.6828	2.367	0.9888	99.44
650	100	0.6109	4.233	0.9976	99.88
1310	10	0.7832	8.371	0.9954	99.77
1310	50	0.7463	9.866	0.9770	98.85
1310	100	0.5412	11.647	0.9329	96.59
1550	10	0.5861	11.128	0.9869	99.34
1550	50	0.8029	10.241	0.9162	95.72
1550	100	0.4960	12.236	0.9756	98.77

At 650 nm the slopes were similar at all three airflow levels (0.61 to 0.68), which means the three lines run almost parallel. What changes is the intercept, which rises from 0.635 at 10% to 2.367 at 50% and 4.233 at 100%.

In practice this is a useful property: the airflow level shifts the whole response upwards by a fairly fixed amount, so the three conditions stay apart at every time point. The quality of fit also improved as the airflow increased, with R^2 going from 0.9651 to 0.9888 and finally 0.9976. The somewhat weaker fit at 10% comes mainly from the slow start of the response, where the readings at 3 s and 6 s are close together before the curve picks up.

The 1310 nm results followed a different pattern. At 10% airflow the response was almost perfectly linear (R^2 = 0.9954), and the intercept again rose with airflow, from 8.371 to 11.647. As the airflow increased, however, the slope fell from 0.7832 to 0.5412 and R^2 dropped to 0.9329 at full fan output. A likely explanation is that strong, turbulent flow drives the fiber into larger and less regular movements. The readings then scatter more around the trend, and the response begins to compress at the top of the range. Even so, all three fits remained well above 0.9.

At 1550 nm the 10% and 100% conditions gave good fits (R^2 of 0.9869 and 0.9756), and the 100% case had the highest intercept of the whole study at 12.236. The 50% condition was the weakest result overall, with R^2 = 0.9162 and a linearity of 95.72%. This dip is almost entirely due to the outlying trial described above. If that one reading is set aside and the 15 s mean is taken from the remaining two trials (20.50), the fit for this condition improves to R^2 = 0.989 with a slope of about 0.590, close to the other two airflow levels. The original value has been kept in Table 4 so that the reported data stay complete, but the check makes clear that the drop at 50% reflects a measurement disturbance and not a basic weakness of the sensor at this wavelength.

Comparison of Wavelengths

Figure 4 sets the R^2 and linearity values side by side. Each wavelength behaves in its own way. At 650 nm both measures improve steadily with airflow, from 98.24% to 99.44% and then 99.88% linearity. At 1310 nm the trend runs the other way, with the best result at low airflow (99.77%) and the poorest at full output (96.59%). At 1550 nm there is a dip at the middle level (95.72%) followed by a recovery to 98.77%. Averaged over the three airflow levels, the mean linearity was 99.19% at 650 nm, 98.40% at 1310 nm and 97.94% at 1550 nm, with matching mean R^2 values of 0.984, 0.968 and 0.960.

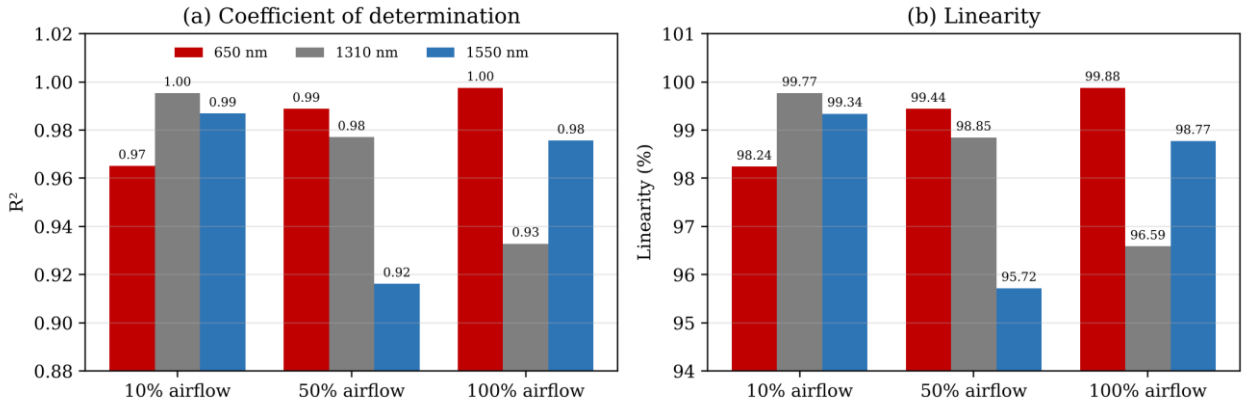

Figure 4: Comparison of (a) R^2 and (b) linearity across wavelengths and airflow levels

Two further observations help to choose between the wavelengths. The first is separation between airflow levels. At 3 s, the 650 nm readings for 10%, 50% and 100% airflow were 3.29, 4.13 and 6.15, a spread of almost 2.9, and the three curves stayed in the same order up to 15 s. At 1550 nm the corresponding readings at 3 s were 13.15, 13.25 and 14.04, a spread of under 0.9, and by 15 s the 10% and 100% curves had effectively merged at about 20.1 to 20.3. At 1310 nm the 50% and 100% curves crossed between 6 s and 9 s, and all three levels converged at about 18 by 12 s. Only the 650 nm source therefore kept the three airflow levels clearly and consistently apart. The second observation is repeatability: the 650 nm data had the smallest trial-to-trial spread, while the single large outlier occurred at 1550 nm.

These points lead to a more balanced conclusion than reading magnitude alone would suggest. The 1550 nm source produced the largest readings and is the natural choice if the sensor must work over long fiber runs, where its lower intrinsic attenuation is an advantage. The 1310 nm source is the most linear at low airflow and would suit applications dominated by gentle flow. For a compact system that needs to tell different airflow levels apart with a simple linear calibration, however, the 650 nm source offers the best overall combination of linearity, level separation and repeatability. It is also the easiest wavelength to work with in practice, since visible red light lets the user see at once whether the fiber is carrying light.

Limitations

Several limitations should be kept in mind. The airflow was described by fan setting rather than by a measured velocity, so the results show relative and not absolute sensitivity; a reference anemometer would be needed to express the response in m/s. The readings were taken as displayed by the OPM, and the relationship between the displayed value and the absolute received power should be confirmed against a no-airflow reference, in line with the referencing schemes recommended by Murtaza and Senior (2000). Each condition was repeated three times over a 15 s window, which is enough to reveal clear trends but too short to describe long-term drift or the time the sensor takes to return to its baseline. Finally, the NodeMCU stage was part of the system design, but the results reported here were recorded with the OPM, so the full wireless monitoring chain still needs to be characterised.

CONCLUSION AND RECOMMENDATIONS

This work developed and tested an airflow detection system based on a stripped single-mode silica fiber that is spliced to a pigtail and read with an optical power meter, with a NodeMCU microcontroller designed in as the processing and wireless stage. The sensor responded to airflow at all three wavelengths tested. Readings rose steadily with exposure time and generally with airflow level, and every condition produced a strong linear fit, with R^2 between 0.9162 and 0.9976. These results show that a simple, low-cost, intensity-modulated fiber sensor that is immune to electromagnetic interference can detect changes in airflow reliably.

The choice of wavelength had a clear effect. The 1550 nm source gave the largest readings but was the least consistent at 50% airflow, and the 1310 nm source was most linear at low airflow but lost some linearity at full fan output. The 650 nm source achieved the highest mean linearity (99.19%), kept the three airflow levels well separated throughout the measurement and showed the best repeatability. On this basis 650 nm is recommended as the operating wavelength for a compact airflow monitoring system of this kind, while 1550 nm remains a sensible option where long fiber lengths are required.

Further work should focus on five areas: calibrating the sensor against a reference anemometer so that its output can be expressed in m/s; improving sensitivity at very low flows by optimising the length and geometry of the stripped section; adding a reference channel or normalisation to cancel source drift and connector loss; completing the NodeMCU stage with cloud-based data logging and alerts for remote monitoring; and exploring machine learning to recognise airflow patterns and anomalies. With these steps, the system has clear commercial potential in HVAC, environmental monitoring, data centres and other industrial settings.

ACKNOWLEDGEMENT

The authors thank the Faculty of Electronics and Computer Technology and Engineering (FTKEK), Universiti Teknikal Malaysia Melaka (UTeM), for providing the laboratory facilities and equipment used in this study.

REFERENCES

1. Azendorf, F., Dochhan, A., & Eiselt, M. H. (2021). Accurate single-ended measurement of propagation delay in fiber using correlation optical time domain reflectometry. Journal of lightwave technology, 39(18), 5744–5752.
2. Diez, S., Lacy, S., Coe, H., Urquiza, J., Priestman, M., Flynn, M., Marsden, N., Martin, N. A., Gillott, S., & Bannan, T. (2024). Long-term evaluation of commercial air quality sensors: an overview from

the QUANT (Quantification of Utility of Atmospheric Network Technologies) study. Atmospheric Measurement Techniques, 17(12), 3809–3827.

3. Espressif Systems. (n.d.). ESP8266EX datasheet. Retrieved January 9, 2026, from https://www.espressif.com/sites/default/files/documentation/0a-esp8266ex_datasheet_en.pdf
4. Jawad, H. J., & Sultan, A. F. (2023). Good cleavers for fiber-optic communication technology. Journal of Optics, 52(2), 468–473.
5. Jay, J. A. (2010). An overview of macrobending and microbending of optical fibers (White Paper WP1212). Corning Optical Communications. https://www.corning.com/media/worldwide/coc/documents/Fiber/white-paper/WP1212.pdf
6. Jiang, Q., Leu, K., Wang, F., Li, R., Wang, K., Zhao, Y., Xi, A., Zang, Y., & Zhang, R. (2025). Structural design and controlled fabrication of advanced airflow sensors. Journal of Materials Chemistry C, 13, 4876–4893. https://doi.org/10.1039/D4TC05127K
7. Johari, S. H., Cheak, T. Z., Abdul Rahim, H. R., Jali, M. H., Mohd Yusof, H. H., Md Johari, M. A., Yasin, M., & Harun, S. W. (2022). ZnO nanorods coated tapered U-shape plastic optical fiber for relative humidity detection. Photonics,
8. KMC Controls. (2025). Smarter airflow measurement: Why traditional methods fall short in performance, cost, and reliability. Building Geniuses. https://www.kmccontrols.com/blog/cap-vs-traditional-airflow-measurement-why-smarter-matters/
9. Konstantatos, G., Clifford, J., Levina, L., & Sargent, E. H. (2007). Sensitive solution-processed visible-wavelength photodetectors. Nature photonics, 1(9), 531–534.
10. Lagakos, N., Cole, J. H., & Bucaro, J. A. (1987). Microbend fiber-optic sensor. Applied Optics, 26(11), 2171–2180. https://doi.org/10.1364/AO.26.002171
11. Lee, J.-R., Dhital, D., & Yoon, D.-J. (2011). Investigation of cladding and coating stripping methods for specialty optical fibers. Optics and lasers in engineering, 49(3), 324–330.
12. Liu, X., Jin, B., Bai, Q., Wang, Y., Wang, D., & Wang, Y. (2016). Distributed fiber-optic sensors for vibration detection. Sensors, 16(8), 1164. https://doi.org/10.3390/s16081164
13. Murtaza, G., & Senior, J. M. (2000). Referencing schemes for intensity modulated optical fiber sensor systems. In K. T. V. Grattan & B. T. Meggitt (Eds.), Optical fiber sensor technology (pp. 303–336). Springer. https://doi.org/10.1007/978-1-4757-6079-8_5
14. The Fiber Optic Association. (n.d.). Termination. In FOA reference for fiber optics. Retrieved January 9, 2026, from https://www.thefoa.org/tech/ref/basic/term.html
15. Yablon, A. D. (2005). Optical fiber fusion splicing. Springer. https://doi.org/10.1007/b137759